



HAL
open science

Elastic modulus of claystone evaluated by nano-/micro-indentation tests and meso-compression tests

Christophe Auvray, Noémie Lafrance, Danièle Bartier

► **To cite this version:**

Christophe Auvray, Noémie Lafrance, Danièle Bartier. Elastic modulus of claystone evaluated by nano-/micro-indentation tests and meso-compression tests. *Journal of Rock Mechanics and Geotechnical Engineering*, 2017, 9 (1), pp.84-91. 10.1016/j.jrmge.2016.02.002 . ineris-01854176

HAL Id: ineris-01854176

<https://ineris.hal.science/ineris-01854176>

Submitted on 31 Aug 2018

HAL is a multi-disciplinary open access archive for the deposit and dissemination of scientific research documents, whether they are published or not. The documents may come from teaching and research institutions in France or abroad, or from public or private research centers.

L'archive ouverte pluridisciplinaire **HAL**, est destinée au dépôt et à la diffusion de documents scientifiques de niveau recherche, publiés ou non, émanant des établissements d'enseignement et de recherche français ou étrangers, des laboratoires publics ou privés.



Contents lists available at ScienceDirect

Journal of Rock Mechanics and Geotechnical Engineering

journal homepage: www.rockgeotech.org

Full Length Article

Elastic modulus of claystone evaluated by nano-/micro-indentation tests and meso-compression tests



Christophe Auvray*, Noémie Lafrance, Danièle Bartier

Université de Lorraine, CNRS, CREGU, Lab. GeoRessources UMR 7359, Vandœuvre-lès-Nancy, F-54518, France

ARTICLE INFO

Article history:

Received 2 November 2015

Received in revised form

21 January 2016

Accepted 9 February 2016

Available online 4 April 2016

Keywords:

Claystone

Elastic modulus

Scaling effect

Nano- and micro-indentation

Meso-compression tests

Multi-scale mechanical tests

ABSTRACT

Toarcian claystone such as that of the Callovo-Oxfordian is a qualified multiphase material. The claystone samples tested in this study are composed of four main mineral phases: silicates (clay minerals, quartz, feldspars, micas) ($\approx 86\%$), sulphides (pyrite) ($\approx 3\%$), carbonates (calcite, dolomite) ($\approx 10\%$) and organic kerogen ($\approx 1\%$). Three sets of measurements of the modulus of deformability were compared as determined in (i) nano-indentation tests with a constant indentation depth of $2 \mu\text{m}$, (ii) micro-indentation tests with a constant indentation depth of $20 \mu\text{m}$, and (iii) meso-compression tests with a constant displacement of $200 \mu\text{m}$. These three experimental methods have already been validated in earlier studies. The main objective of this study is to demonstrate the influence of the scaling effect on the modulus of deformability of the material. Different frequency distributions of the modulus of deformability were obtained at the different sample scales: (i) in nano-indentation tests, the distribution was spread between 15 GPa and 90 GPa and contained one peak at 34 GPa and another at 51 GPa; (ii) in the micro-indentation tests, the distribution was spread between 25 GPa and 60 GPa and displayed peaks at 26 GPa and 37 GPa; and (iii) in the meso-compression tests, a narrow frequency distribution was obtained, ranging from 25 GPa to 50 GPa and with a maximum at around 35 GPa.

© 2017 Institute of Rock and Soil Mechanics, Chinese Academy of Sciences. Production and hosting by Elsevier B.V. This is an open access article under the CC BY-NC-ND license (<http://creativecommons.org/licenses/by-nc-nd/4.0/>).

1. Introduction

Understanding the mechanical behaviour of claystone is of critical importance for nuclear waste storage. Previous studies of this material have mostly focused on its mechanical properties at the macroscopic scale. The tests were generally performed on 20 mm or 38 mm diameter cylindrical samples with a length to width ratio of 2, given that the sample lengths are 40 mm and 76 mm, respectively (Chiarelli et al., 2003; Shao et al., 2006; Hoxha et al., 2007; Jia et al., 2010). Micro-macromechanical approaches linked to macroscopic tests have also been attempted on this material, most notably in the study of Shen et al. (2012).

In order to better understand the instantaneous mechanical behaviour of the claystone at different sample scales, we conducted three series of measurements for this study: (i) nano-indentation tests, in which the volume of material tested each time was around 0.001 mm^3 ; (ii) micro-indentation tests, in which around 1 mm^3 of material was tested; and (iii) meso-compression tests, performed on around 250 mm^3 of material. The representative elementary volume

(REV) of the material is in the order of 0.001 mm^3 (Robinnet, 2008; Robinnet et al., 2012). Consequently, a single nano-indentation measurement takes into account only one REV, and in contrast, a meso-compression test requires a sample with a volume of 1×10^6 REV.

The experimental techniques adopted for the three types of tests have already been validated on other materials: (i) Callovo-Oxfordian claystone from the ANDRA Underground Research Laboratory (URL) at Meuse/Haute-Marnes (France), on which both nano- (Magnenet et al., 2011a,b; Auvray et al., 2013, 2015; Arnold et al., 2015) and micro-indentation (Magnenet et al., 2009) tests were performed; and (ii) iron minerals from underground mines in Moselle (France), and (iii) limestone quarries in Lavoux (France), on which micro- and meso-compression tests were performed (Grgic et al., 2013).

In the present study, the values of the moduli of deformability measured in the tests performed at the three different scales were compared in order to quantify the modulus-volume relationship.

2. Multi-scale mechanical tests

2.1. Typical characteristics of the rock materials

The claystone samples studied are a qualified multiphase material composed of four principal mineral phases: silicates of about

* Corresponding author. Tel.: +33 0383596301.

E-mail address: christophe.auvray@univ-lorraine.fr (C. Auvray).

Peer review under responsibility of Institute of Rock and Soil Mechanics, Chinese Academy of Sciences.

86% (clays, 55%; quartz, 19%; feldspars/micas, 12%), sulphides of about 3% (pyrite), carbonates of about 10% (calcite, dolomite), and a form of organic kerogen of about 1% (Niandou, 1994; Schmitt et al., 1994; Niandou et al., 1997; Charpentier et al., 2001, 2004; Tinseau et al., 2006; Savoye et al., 2008).

The typical physical properties of the claystone are given in Table 1 (Niandou, 1994; Schmitt et al., 1994; Niandou et al., 1997; Chiarelli et al., 2003; Zhang and Rothfuchs, 2004).

2.2. Experimental equipment

The technical specifications of the nano- and micro-indentation testers and mini-compression (triaxial) cell are provided in Table 2.

2.2.1. Nano-indentation press

The nano-indentation apparatus consists of two cells, one of which contains the nano-indenter (CSM-Instruments) and the other contains an optical microscope for viewing the surface of the sample (Fig. 1).

For the nano-indentation tests, the surfaces of the sample must be as flat and as smooth as possible and must lie parallel to the support-stage axes. The distance between the support-stage plane and the indented surface must not vary by more than 5 μm . Though these requirements are systematic when preparing samples for indentation tests, it is particularly important that they are adhered to each other for the nano-indentation experiments (Vandamme, 2008; Miller et al., 2008; Auvray et al., 2015).

The experimental procedure used in this study was developed by the GeoResources Laboratory (Nancy, France) and was presented in Auvray et al. (2013, 2015). The indentation procedure consists of pressing an indenter into the surface of a sample by applying an increasing normal load. The procedure is performed in a repetitive manner at different points on the sample surface at a constant interval along both the x - and y -axis. The load is directly applied by an electromagnet assembly attached to a vertical rod, the end of which houses a standard Berkovich diamond indenter. Displacement of the rod is measured by a capacitive detector and the rod is supported by two guide springs (Randall et al., 1997).

2.2.2. Micro-indentation press

In the nano-indentation tests, the surfaces of the sample must be flat and smooth. The experimental procedure used in this study was presented in detail in Magnenet et al. (2011b) and Grgic et al. (2013). In brief, the indentation procedure involves pressing an

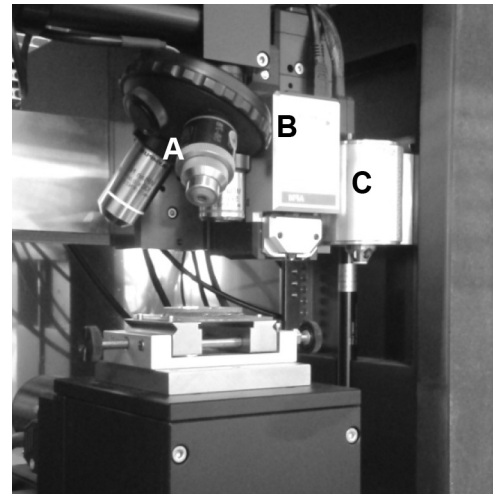


Fig. 1. Nano-indentation tester (A: Optical microscope, B: Atomic force microscope, C: Nano-indenter).

indenter into the surface of a sample by applying an increasing normal load.

The micro-indentation press (Agotech) is equipped with a 5000-N force sensor. The piston holds a flat indenter tip made of tungsten carbide. The chosen size of the indenter tip ($\phi = 0.5 \text{ mm}$) is representative of the micro-structure of the claystone. The size of the REV is 0.1 mm (Robinet, 2008; Robinet et al., 2012). The penetration depth corresponds to the mean value of the displacements, as measured using two LVDT sensors, and the force is measured with a force sensor positioned on the axis of the indenter tip (Fig. 2).

2.2.3. The compression cell

Meso-scale uniaxial compression tests were performed on centimetre-scale cylindrical samples ($h = 10 \text{ mm}$, $\phi = 5 \text{ mm}$) with a loading rate of 0.25 MPa/min. A mini-triaxial cell was developed in the laboratory for the meso-compression tests (Fig. 3). The experimental procedure used in this study was presented in detail in Grgic et al. (2013). In this assembly, the confining fluid is prevented from penetrating the rock specimen by means of a flexible sleeve placed around the cylindrical sample. The confining pressure is zero as the tests are essentially uniaxial compression tests. A self-compensated axial piston is used, and the cell is autonomous and does not require an external load press. Axial and transverse deformations were measured using four extensometers. Two of the gauges were diametrically opposed and used to measure axial deformation, and the other two gauges were used for measuring transverse deformation.

2.3. Equations for the modulus of deformability

The model of Oliver and Pharr (1992, 2004) was used for the nano- and micro-indentation tests. This model allows the Young's modulus (E_{it}) of the indented zone to be derived from load–

Table 1

Typical physical properties of the material tested.

ρ_b (g/cm ³)	ρ_d (g/cm ³)	ρ_s (g/cm ³)	n (%)	w (%)
2.38–2.41 ^a	2.18–2.27 ^a	2.68–2.73 ^c	4–9 ^{a-d}	11–15 ^{a,b}

Note: ρ_b : bulk density; ρ_d : dry density; ρ_s : skeletal density; n : total porosity; w : natural water content.

^a Zhang and Rothfuchs, 2004.

^b Chiarelli et al., 2003.

^c Niandou, 1994; Niandou et al., 1997.

^d Schmitt et al., 1994.

Table 2

Technical specifications.

Testing device	Load range (N)	Load resolution (N)	Maximum depth (mm)	Depth resolution (mm)	Maximum load rate (N/s)	Indenter
Indentation tester	0.001–0.500	4.0×10^{-8}	0.2	4.0×10^{-8}	4.0×10^{-3}	Berkovich
Micrope tester	0.1–5000	1.0×10^{-5}	2.5	0.01	0.5	Flat ($\phi = 0.5 \text{ mm}$)
Mini-triaxial cell	1–20,000	0.1	2.5	0.01	5	–

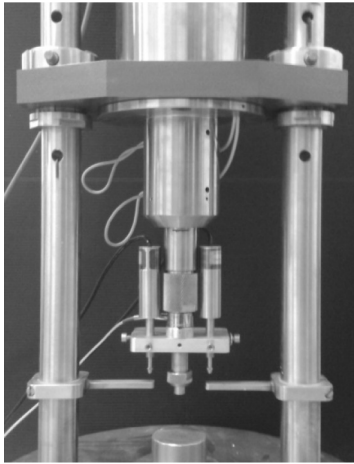


Fig. 2. Micro-indentation tester.

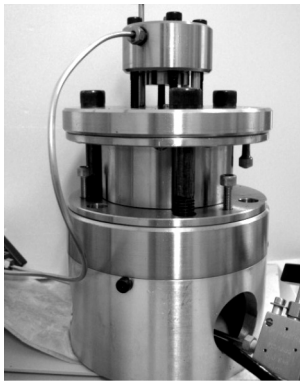


Fig. 3. Mini-triaxial cell.

displacement curves (Fig. 4), using the equation for the reduced modulus, E_r :

$$E_r = \frac{s\sqrt{\pi}}{2\beta\sqrt{A_p(h_c)}} \quad (1)$$

where s is the elastic unloading stiffness, defined as the tangent of the unloading curve; β is a correction factor related to the geometry of the indenter; $A_p(h_c)$ is the projected contact area of the indentation as a function of the contact depth; and h_c can be obtained from

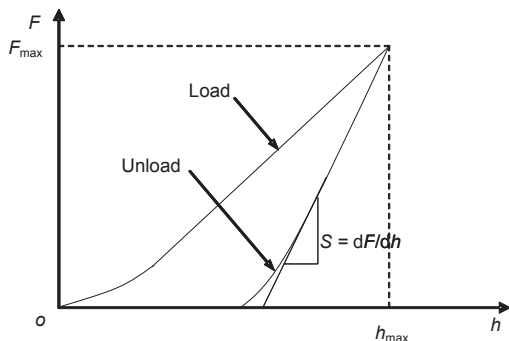


Fig. 4. Nano- and micro-indentation tests – typical load–displacement curve.

$$h_c = h_{max} - \alpha \frac{F_{max}}{S} \quad (2)$$

where F_{max} is the load value before unloading and α is a coefficient that depends on the indenter geometry.

From a theoretical point of view, the tangent ($S = df/dh$) is calculated between the start of the unloading phase and the end of the linear part of this phase, as shown in Fig. 4. In order to ensure repeatability and avoid any variability in the measurement of the slope S in our tests, the tangent was systematically measured between the start of the unloading phase and 50% of the unloading.

The Young's modulus of the indented material is then obtained using:

$$\frac{1}{E_r} = \frac{1 - \nu_{it}^2}{E_{it}} + \frac{1 - \nu_i^2}{E_i} \quad (3)$$

where ($E_i = 1141$ GPa) and ($\nu_i = 0.07$) are the elastic modulus and Poisson's ratio of the indenter, respectively; ν_{it} and E_{it} are the Poisson's ratio and modulus of deformability of the indentation zone, respectively.

According to the earlier experimental and numerical studies in which experimental conditions were applied, the mean Poisson's coefficient attributed to this material is equal to 0.30 (Niandou, 1994; Niandou et al., 1997; Homand et al., 2006; Kazmierczak et al., 2008; Magnenet et al., 2011a,b; Auvray et al., 2015).

In the meso-compression tests, the modulus of deformability (E) is derived from strain-deformation curves (Fig. 5) using the following equation in accordance with the NF P94-425-2002 (2002) standard:

$$E = \frac{\Delta(\sigma_1 - \sigma_3)}{\Delta\epsilon_a} \quad (4)$$

where $(\sigma_1 - \sigma_3)$ represents the deviatoric stress in triaxial configuration of revolution (in this case, $\sigma_3 = 0$) and ϵ_a corresponds to the mean axial deformation recorded by the gauges.

2.4. Measurement protocols

The test programme consisted of three series of measurements (nano- and micro-indentation tests and meso-compression tests). The number of tests performed in each measurement campaign depended on the different volumes of materials required for each test and on the limited amount of materials available. In total, 520 nano-indentation tests, 221 micro-indentation tests, and 21 meso-compression tests were performed. To avoid any hydromechanical coupling, tests were performed on partially desaturated material, achieved by storing samples in atmosphere with 30% humidity for

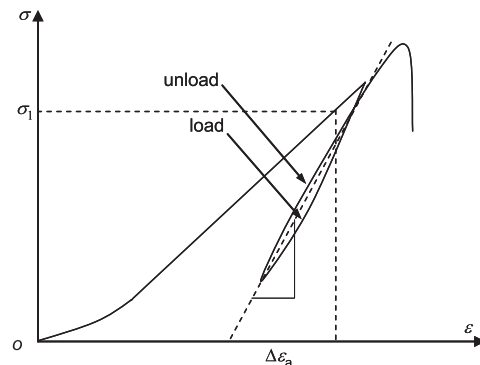


Fig. 5. Typical stress-axial strain curves of meso-compression test.

three months prior to testing. These partial desaturation experimental conditions have already been applied in a number of experimental campaigns, notably in Shao et al. (2006) and Hoxha et al. (2007). Because of the limited amount of materials available for the present study, tests could only be conducted with the stress direction perpendicular to the plane of anisotropy (plane 2–3 in Fig. 6), which corresponds to the stratification plane. The indentation and deformation measurements were therefore also made perpendicular to this plane.

The nano-indentation tests were conducted using the following parameters:

- (1) Loading and unloading rate of 0.03 N/min, and
- (2) Measurement of the elastic modulus at a constant depth of 2 μm.

For the micro-indentation tests, the parameters were:

- (1) Loading and unloading rate of 30 N/min, and
- (2) Measurement of the elastic modulus at a constant depth of 20 μm.

Finally, the following parameters were used for the meso-compression tests:

- (1) Loading and unloading rate of 100 N/min, and
- (2) Measurement of the elastic modulus with constant displacement of 200 μm.

In the indentation tests (nano or micro), any variation in the indentation depth will likely result in a variation in the modulus,

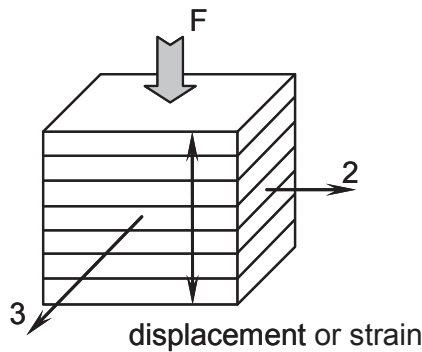


Fig. 6. Displacement or strain in relation to the anisotropic structure of argillite.

because plasticity or damage can be induced when the penetration depth is too large. In order to avoid this, we used preliminary tests to determine the maximum depth at which the mechanical behaviour remained solely elastic, and then fixed the indentation depth at this value.

Similarly, for the meso-compression tests, preliminary tests were conducted to allow us to determine the boundary between elastic and plastic behaviours. We fixed the amount of displacement used for measuring the modulus at this limit.

3. Results and interpretation

Histograms of the modulus values and F/F_m coefficients (F is the maximum force reached during any given individual test; F_m is the maximum force reached in all of the tests considered) were calculated for each set of tests.

Statistical analyses were performed according to the method proposed by Constantinides et al. (2006). The cumulative distribution function Φ_{exp} was fitted by superimposition of three normal distributions Φ_k (with $k = 1, 2, 3$) with mean value μ_k , standard deviation σ_k , volume fraction f_k , and Gauss function error erf , which can be written as

$$\Phi_k^i = \frac{1}{\sqrt{2\pi}} f_k \int_{-\infty}^{\frac{x_i - \mu_k}{\sigma_k}} e^{-\frac{t^2}{2}} dt = \frac{1}{2} f_k \left[1 + erf\left(\frac{x_i - \mu_k}{\sigma_k \sqrt{2}}\right) \right] \quad (5)$$

The decision to use three phases was operator-dependent, and reflected the composition of the claystone by optical microscopy (Fig. 7): (i) a weak phase likely corresponding to the clayed matrix; (ii) an intermediate phase in which the clayed matrix had been hardened in the presence of hard micro-inclusions; and (iii) a hard phase corresponding to the largest hard inclusions.

The optimization algorithm consisted of minimizing the cost function ϵ , as defined by

$$\epsilon(\mathbf{P}) = \left\| \Phi_{exp} - \sum_{k=1}^3 \Phi_k^i \right\| \quad (6)$$

where \mathbf{P} is the vector of parameters to be optimized; f_k ($k = 1, 2, 3$) is the parameter satisfying the constraint $f_1 + f_2 + f_3 = 1$. This enabled determination of the mean values and standard deviation of each normal distribution, as well as their volume fractions. The frequency distributions of the elastic moduli and F/F_m of the three series of tests are shown in Figs. 8 and 9, respectively.

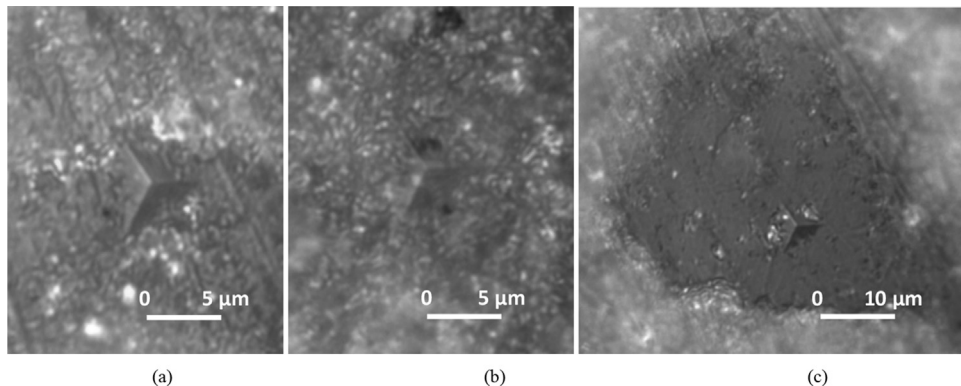


Fig. 7. Photographs of indents in argillaceous matrix containing micro- and macro-inclusions (<1 μm in size) of calcite and quartz. (a) Matrix with a low proportion of micro-inclusions; (b) Matrix with a high proportion of micro-inclusions; and (c) Matrix containing a calcite macro-inclusion (approximately 30 μm in size).

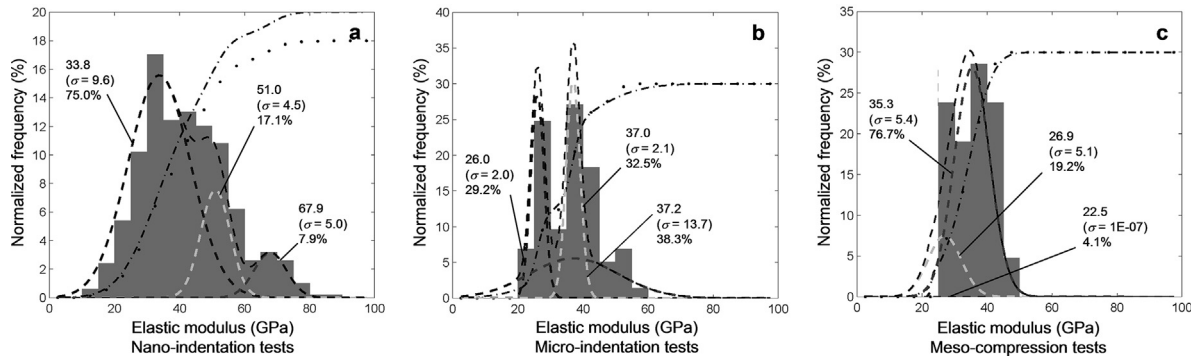


Fig. 8. Experimental frequency distributions of elastic modulus for (a) nano-indentation, (b) micro-indentation, and (c) meso-compression tests.

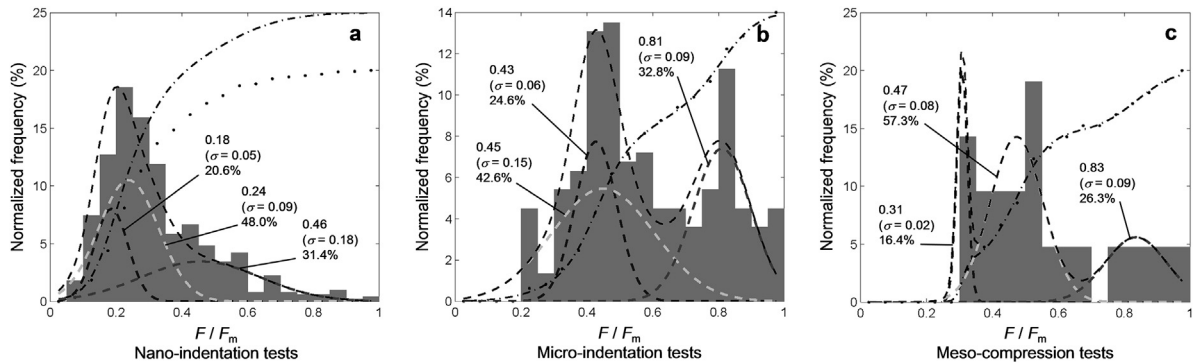


Fig. 9. Experimental frequency distributions of F/F_m in (a) nano-indentation, (b) micro-indentation, and (c) meso-compression tests.

3.1. Test results

3.1.1. Results of nano-indentation tests (see Figs. 8a and 9a)

- (1) The elastic modulus distribution shows a relatively wide spread of values between 15 GPa and 90 GPa. The distribution is bimodal and positively skewed shape, with a large peak apparent at around 34 GPa and a smaller peak at around 51 GPa.
- (2) The F/F_m frequency distribution ranges from 0 to 1.0, with a maximum centred at 0.24.

3.1.2. Results of micro-indentation tests (see Figs. 8b and 9b)

- (1) The distribution of the elastic modulus is narrower than it was for the nano-indentation tests. Values are spread between 20 GPa and 60 GPa, and two peaks are located at around 26 GPa and 37 GPa.
- (2) The F/F_m distribution is spread between 0.20 and 1.0 and contains two peaks at 0.43–0.45 and 0.81, respectively.

3.1.3. Results of meso-compression tests (Figs. 8c and 9c)

- (1) The distribution of the elastic modulus is very tight, ranging from 25 GPa to 50 GPa with a maximum observed at around 35 GPa.
- (2) The F/F_m distribution ranges from 0.30 to 1.0, with two peaks located at 0.47 and 0.83, respectively.

3.2. Comparison and interpretation

3.2.1. Different distributions of various scale tests

Given the distribution of the clayed matrix and isotropic hard inclusions at the macroscopic scale, we assumed that three

different phases are distributed similarly at each scale. As such, the different distributions can be compared and interpreted as follows:

- (1) At the nano-indentation scale, three families of measurements (Fig. 8a) can be distinguished. These three families most likely represent the modulus values for a matrix of variable purity, for a matrix containing variable numbers of micro-inclusions, and finally, for zones containing little matrix and variable numbers of inclusions.
- (2) At the micro-indentation scale, three families of moduli are less well-defined (Fig. 8b). The matrices appear to contain variable amounts of micro-inclusions as well as a number of larger inclusions.
- (3) At the meso-compression scale, the modulus distribution is very tight (Fig. 8c). Even though peaks at 27 GPa, 35 GPa, and 22.5 GPa can be distinguished, the multimodal distribution observed at the nano- and micro-indentation scales is much less apparent. The matrix again appears to be associated with micro-inclusions. Only the proportion of large inclusions present appears to vary.
- (4) A tightening of the elastic modulus frequency distributions with increasing sample size is apparently observed (Fig. 10), and is most likely due to the fact that the nano-indentation tests allow both the elastic moduli of certain inclusions and the modulus of a pure clayed matrix to be measured. This was also observed in the study of Auvray et al. (2015) and a number of hypotheses were put forward to explain it. Constantinides et al. (2006) and Constantinides and Ulm (2007) showed that the statistical processing of nano-indentation tests is only relevant if the typical size of the inclusions (d) is much larger than the typical penetration depth (h). If $d \ll h$, the material can be considered

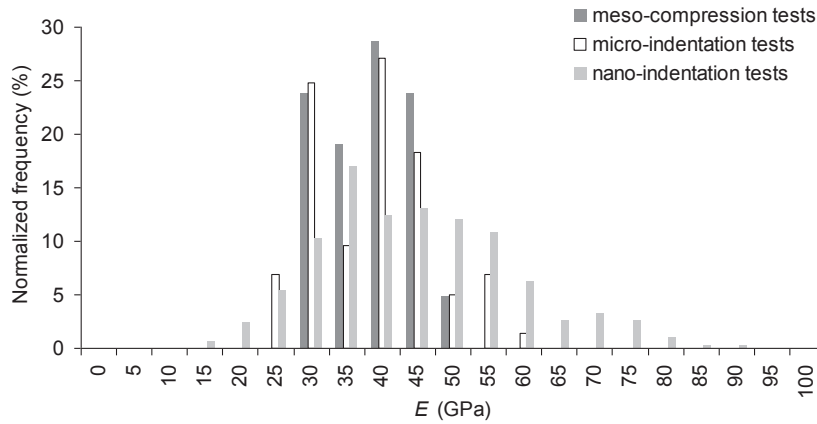


Fig. 10. Variability in elastic modulus with the types of tests.

homogeneous (see Fig. 2, in Constantinides and Ulm, 2007); whereas when $d \gg h$, the mechanical behaviour of the individual constituent becomes important. The choice of the indentation depth for this claystone was particularly problematic because of the wide range of inclusion sizes presented and the limited number of specimens available. Two characteristic inclusion sizes could be identified from optical microscopy, the smallest of which was approximately $1 \mu\text{m}$. According to Tinseau et al. (2006), the largest inclusions appear to be greater than $50 \mu\text{m}$. Conversely, the clayed matrix is itself composed of different clay minerals as well as minute hard inclusions of micrometric size. In previous studies, the “ $1 \mu\text{m} < h < 10 \mu\text{m}$ ” condition was met for all of these heterogeneities (Magnenet et al., 2011a; Auvray et al., 2015). The fixed indentation depth of $2 \mu\text{m}$ used for the nano-indentation tests in this study thus allowed all of the phases presented in the material to be indented.

3.2.2. F/F_m coefficients of various scale tests

Assuming once more that the material is homogenous at macro-scale, the distributions of the F/F_m coefficients can be compared and interpreted as follows:

- (1) At the nano-indentation scale, we observe a very wide distribution of F/F_m values (Fig. 9a), synonymous with significant variation in the maximum force reached in each measurement. This may suggest indentation of different

phases (e.g. clay minerals, micro-inclusions or larger inclusions) during each measurement.

- (2) At the micro-indentation scale, the distribution is wider again and two peaks can easily be distinguished (Fig. 9b). The peak at 0.43 may correspond to the zones that contain only micro-inclusions, and the peak at 0.81 might represent the zones that are richest in inclusions. The general distribution from 0.20 to 1.00 with a peak at 0.45 may be representative of a matrix that contains variable amounts of micro-inclusions and larger inclusions.
- (3) At the meso-compression scale (Fig. 9c), three peaks (0.31, 0.47, and 0.83) can be distinguished. These are associated with samples that all contain large inclusions but that contain different amounts of micro-inclusions.
- (4) There is a significant narrowing and shift of the F/F_m coefficient distributions with increasing sample size (Fig. 11). This most likely indicates that the maximum force reached during each measurement depends on the proportion of micro-inclusions and larger inclusions presented.

4. Discussion

The elastic modulus of the Toarcian claystone appears to be strongly dependent on the volume of sample tested. This is consistent with the multiphase nature of the material, which is composed of a heterogeneous matrix containing both micro-inclusions and larger inclusions. This would in turn suggest that the elastic modulus of a monophasic material, such as a pure silica,

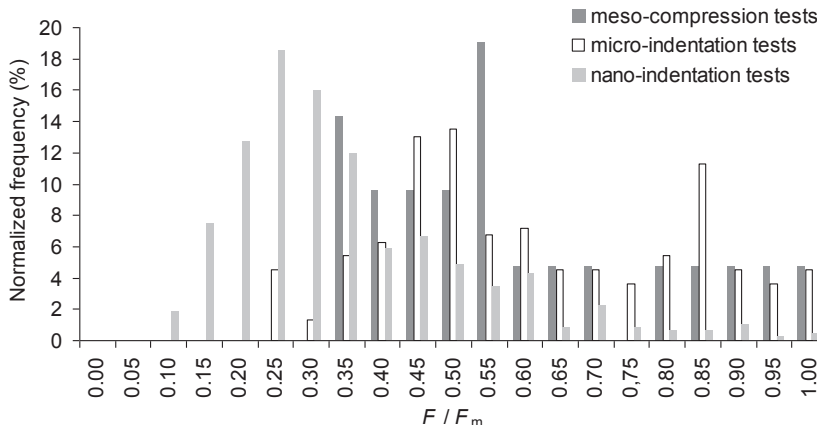


Fig. 11. Variability in the F/F_m coefficients with the types of tests.

or even a polymer or a pure metal, is the same whatever the scale of the samples tested (nano-, micro-, meso- or macroscopic) is. In such cases, the parameter could therefore be considered intrinsic to the material (Doerner and Nix, 1986; Rodriguez and Gutierrez, 2003; Shuman et al., 2007; Oliveira et al., 2014).

On the basis of our results, and in discarding the concept of damage, elastic moduli obtained from a multimillimetric sample most likely cluster around a value of 30 GPa or less. This is supported in part by the studies of Niandou (1994), Niandou et al. (1997), Rejeb (1999), Valès et al. (2004), and Masri et al. (2014), in which elastic moduli of 20–35 GPa were determined from uniaxial compression and compressibility tests carried out on cylindrical samples of 38 mm in diameter and cubes of 50 mm in width.

The present study highlights the advantages of conducting tests on small sample volumes in order to determine the elastic modulus of each constituent phase in a material (particularly when only samples of small size are available). The elastic moduli can then be interpreted in terms of the mineralogical and structural complexity of the sample, and these parameters can subsequently be incorporated into micro/macro-mechanical behaviour models developed within the framework of homogenization of random heterogeneous media theory as applied to multi-scale porous materials (Kachanov and Sevostianov, 2005; Sevostianov et al., 2008; Hashemia et al., 2009; McCartney, 2010; Sevostianov and Giraud, 2012, 2013). A number of semi-analytical, analytical and numerical approaches are currently being explored. As a result of recent advances in analytical, experimental and numerical techniques, fundamental scientific questions concerning the micro/macro-mechanical behaviours of materials can now be addressed. These results will eventually be integrated into finite element numerical codes dedicated to the modelling of underground structures (storage sites, mines, etc.). To the best of our knowledge, applications to underground structure calculations are at present almost non-existent. This research will provide a better understanding of the influence of microstructure on the short- and long-term macroscopic behaviours of materials at the laboratory and in-situ scale.

5. Conclusions

The main objective of this study is to demonstrate the effect of scaling on the modulus of deformability of a specific type of material, a Toarcian claystone. Different elastic modulus frequency distributions were obtained for the different volumes of samples tested:

- (1) At the nano-indentation scale, we were able to identify three families of elastic moduli. The first corresponded to the modulus of the pure clayed matrix, the second to a matrix containing micro-inclusions, and the last to a matrix containing larger inclusions.
- (2) At the micro-indentation scale, three families could again be distinguished, but this time with more difficulty. The three groups corresponded to the moduli of a matrix containing variable proportions of large inclusions.
- (3) At the meso-compression scale, a unimodal frequency distribution for the moduli was observed and it was difficult to distinguish any particular families. The measured values all appeared to correspond to a clayed matrix containing large inclusions and variable proportions of micro-inclusions.

The observed variability in the elastic modulus can thus be explained by the multiphase nature of the material, which contains both micro-inclusions and inclusions of larger size. The elastic modulus of a monophasic material should therefore be the same at

all scales of investigation (nano-, micro-, meso- or macroscopic), and the parameter could in such a case be considered to be intrinsic to the material.

The results of this study demonstrate the importance of having a thorough knowledge of the lithology and mineralogy of the material to be tested. It is clear that the structure of the material must also be observed at the different scales of the tests conducted. Without such information, the variability in the elastic modulus would be difficult to interpret and the use of this parameter in micro- or macro-mechanical behaviour models would remain limited.

Conflict of interest

The authors wish to confirm that there are no known conflicts of interest associated with this publication and there has been no significant financial support for this work that could have influenced its outcome.

Acknowledgements

The authors would like to thank the GNR NEEDS-MIPOR for funding this project.

References

- Arnold G, Auvray C, Giraud A, Armand G. Claystone phases mechanical properties identified from temperature and humidity controlled nano-indentation measurements. In: ISRM Congress 2015. Proceedings of the International Symposium on Rock Mechanics. Montréal Canada; 2015.
- Auvray C, Giot R, Grgic D. Nano-indentation partially saturated argillite: experience device and measurements. In: Proceedings of EUROCK 2013. Rock Mechanics for Resources, Energy and Environment – The 2013 ISRM European Rock Mechanics Symposium. Wrocław Poland: A.A. Balkema; 2013. p. 201–5.
- Auvray C, Arnold G, Armand G. Experimental study of elastic properties of different constituents of partially saturated argillites using nano-indentation tests. *Engineering Geology* 2015;191:61–70.
- Charpentier D, Cathelineau M, Mosser-Ruck R, Bruno G. Mineralogical evolution of argillites in dehydrated-oxidised zones: the example of the argillitic walls from Tournemire tunnel. *Comptes Rendus de l'Académie des Sciences – Series IIA – Earth and Planetary Science* 2001;332(10):601–7.
- Charpentier D, Mosser-Ruck R, Cathelineau M, Guillaume D. Oxidation of mudstone in a tunnel (Tournemire, France): consequences for the mineralogy and crystal chemistry of clay minerals. *Clay Minerals* 2004;39(2):135–49.
- Chiarelli AS, Shao JF, Hoteit N. Modeling of elastoplastic damage behavior of a claystone. *International Journal of Plasticity* 2003;19(1):23–45.
- Constantinides G, Ulm FJ. The granular nature of C-S-H. *Journal of the Mechanics and Physics of Solids* 2007;55(1):64–90.
- Constantinides G, Ravi Chandran KS, Ulm FJ, van Vliet KJ. Grid indentation analysis of composite microstructure and mechanics: principles and validation. *Materials Science and Engineering: A* 2006;430(1/2):189–202.
- Doerner MF, Nix WD. A method for interpreting the data from depth-sensing indentation instruments. *Journal of Materials Research* 1986;1(4):601–9.
- Grgic D, Giraud A, Auvray C. Impact of chemical weathering on micro/macro-mechanical properties of oolitic iron ore. *International Journal of Rock Mechanics and Mining Sciences* 2013;64:236–345.
- Hashemia R, Avazmohammadia R, Shodjabc HM, Weng GJ. Composites with superspherical inhomogeneities. *Philosophical Magazine Letters* 2009;89:439–51.
- Homand F, Shao JF, Giraud A, Auvray C, Hoxha D. Petrofabric and mechanical properties of mudstones. *Comptes Rendus de l'Académie des Sciences – Series IIA – Earth and Planetary Science* 2006;338(12–13):882–91.
- Hoxha D, Giraud A, Homand F, Auvray C. Saturated and unsaturated behaviour modelling of Meuse-Haute-Marne argillite. *International Journal of Plasticity* 2007;23(5):733–66.
- Jia Y, Bian H, Su K, Kondo D, Shao J. Elastoplastic damage modelling of desaturation and resaturation in argillites. *International Journal for Numerical and Analytical Methods in Geomechanics* 2010;34(2):187–220.
- Kachanov M, Sevostianov I. On quantitative characterization of microstructures and effective properties. *International Journal of Solids and Structures* 2005;42(2):309–36.
- Kazmierczak JB, Laoufa F, Ghoreychin M, Lebon P, Barnichon JD. Influence of creep on water pressure measured from borehole tests in the Meuse/Haute-Marne Callovo-Oxfordian argillites. *Physics and Chemistry of the Earth (Parts A/B/C)* 2008;32(8–14):917–21.

- Magnenet V, Auvray C, Djordem S, Homand F, Giraud A. On the estimation of elastoplastic properties of rocks by indentation tests. *Internal Journal of Rocks Mechanics and Mining Sciences* 2009;46(3):635–42.
- Magnenet V, Giraud A, Auvray C. About the effect of relative humidity on the indentation response of Meuse/Haute-Marne argillite. *Acta Geotechnica* 2011a;6(3):155–66.
- Magnenet V, Auvray C, Francius G, Giraud A. Determination of the matrix indentation modulus of Meuse/Haute-Marne argillite. *Applied Clay Science* 2011b;52(3):266–9.
- Masri M, Sibai M, Shao JF, Mainguy M. Experimental investigation of the effect of temperature on the mechanical behavior of Tournemire shale. *International Journal of Rock Mechanics and Mining Sciences* 2014;70:185–91.
- McCartney LN. Maxwell's far-field methodology predicting elastic properties of multiphase composites reinforced with aligned transversely isotropic spheroids. *Philosophical Magazine* 2010;90(31/32):4175–207.
- Miller M, Bokko C, Vandamme M, Ulm FJ. Surface roughness criteria for cement paste nano-indentation. *Cement and Concrete Research* 2008;38(4):467–76.
- Niandou H. Etude du comportement rhéologique et modélisation de l'argilite de Tournemire: applications à la stabilité d'ouvrages souterrains. Ph.D. Thesis. Lille: University of Lille, France; 1994 (in French).
- Niandou H, Shao JF, Henry JP, Fourmaintraux D. Laboratory investigation of the mechanical behaviour of Tournemire shale. *International Journal of Rocks Mechanics and Mining Sciences* 1997;34(1):3–16.
- NF P94-425-2002. Rock – determination of the Young modulus and the Poisson's ratio. La Plaine Saint-Denis Cedex, France: Association Francaise de Normalisation (NF); 2002 (in French).
- Oliveira GL, Costa CA, Teixeira SCS, Costa MF. The use of nano- and micro-instrumented indentation tests to evaluate viscoelastic behavior of poly (vinylidene fluoride) (PVDF). *Polymer Testing* 2014;34:10–6.
- Oliver WC, Pharr GM. An improved technique for determining hardness and elastic modulus using load and displacement sensing indentation experiments. *Journal of Materials Research* 1992;7(6):1564–83.
- Oliver WC, Pharr GM. Measurement of hardness and elastic modulus by instrumented indentation: advances in understanding and refinements to methodology. *Journal of Materials Research* 2004;19(1):3–20.
- Randall NX, Julia-Schmutz C, Soro JM, von Stebut J, Zacharie G. Novel nano-indentation method for characterising multiphase materials. *Thin Solid Films* 1997;308–309:297–303.
- Rejeb A. Mechanical characterisation of the argillaceous Tournemire site (France). In: Jha PC, Gupta RN, editors. *Proceedings of the International Conference on Rock Engineering Techniques for Site Characterisation*. Bangalore, India: Oxford Press; 1999.
- Robinet JC. Minéralogie, porosité et diffusion des solutés dans l'argilite du Callovo-Oxfordien de Bure (Meuse/Haute-Marne, France) de l'échelle centimétrique à micrométrique. Ph.D. Thesis. Poitiers: Université de Poitiers; 2008 (in French).
- Robinet JC, Sardini P, Coelho D, Parneix J, Pret D, Sammartino S, Boller E, Altmann S. Effects of mineral distribution at mesoscopic scale on solute diffusion in a clay-rich rock: example of the Callovo-Oxfordian mudstone (Bure, France). *Water Resources Research* 2012;48(5):W05554. <http://dx.doi.org/10.1029/2011WR011352>.
- Rodriguez R, Gutierrez I. Correlation between nanoindentation and tensile properties influence of the indentation size effect. *Materials Science and Engineering: A* 2003;361(1/2):377–84.
- Savoye S, Michelot JL, Altinier MV, Lemius S. Origin of pore-water isotopic anomalies near fractures in the Tournemire shales. *Physics and Chemistry of the Earth, Parts A/B/C* 2008;33(Suppl. 1):S87–94.
- Schmitt L, Forsans T, Santarelli FJ. Shale testing and capillary phenomena. *International Journal of Rock Mechanics and Mining Sciences & Geomechanics Abstracts* 1994;31(5):411–27.
- Sevostianov I, Giraud A. On the compliance contribution tensor for a concave superspherical pore. *International Journal of Fracture* 2012;177(2):199–206.
- Sevostianov I, Giraud A. Generalization of Maxwell homogenization scheme for elastic material containing inhomogeneities of diverse shape. *International Journal of Engineering Science* 2013;64:23–36.
- Sevostianov I, Kachanov M, Zohdi T. On computation of the compliance and stiffness contribution tensors of non-ellipsoidal inhomogeneities. *International Journal of Solids and Structures* 2008;45(16):4375–83.
- Shao J, Jia Y, Kondo D, Chiarelli AS. A coupled elastoplastic damage model for semi-brittle materials and extension to unsaturated conditions. *Mechanics of Materials* 2006;38(3):218–32.
- Shen WQ, Shao JF, Kondo D, Gatmiri B. A micro-macro model for clayey rocks with a plastic compressible porous matrix. *International Journal of Plasticity* 2012;36:64–85.
- Shuman DJ, Costa ALMb, Andrade MS. Calculating the elastic modulus from nano-indentation and microindentation reload curves. *Materials Characterization* 2007;58(4):380–9.
- Tinseau E, Bartier D, Hassouta L, Devol-Brown I, Stammose D. Mineralogical characterization of the Tournemire argillite after in situ interaction with concretes. *Waste Management* 2006;26(7):789–800.
- Valès F, Nguyen Minh D, Gharbi H, Rejeb A. Experimental study of the influence of the degree of saturation on physical and mechanical properties in Tournemire shale (France). *Applied Clay Science* 2004;26(1/4):197–207.
- Vandamme M. The nanogranular origin of concrete creep: a nano-indentation investigation of microstructure and fundamental properties of calcium-silicate-hydrate. Ph.D. Thesis. Cambridge, USA: Massachusetts Institute of Technology; 2008.
- Zhang C, Rothfuchs T. Experimental study of the hydro-mechanical behaviour of the Callovo-Oxfordian argillite. *Applied Clay Science* 2004;26(1/4):325–36.



Christophe Auvray has a background in hydrogeomechanics, geotechnics and civil engineering (Master, University of Québec – Chicoutimi, UQAC, speciality: hydrogeomechanics). In 2003, he obtained his PhD from the University of Lorraine (Nancy, France): “Rheological behaviour of gypsum quarries”. Today, he is a research engineer at the GeoResources Laboratory (Vandoeuvre-Les-Nancy, France) and is in charge of conducting field experiments in geomechanics. His main field of research is in the multi-scale experimental characterization of THMC coupled behaviour in rocks. Applications of this include laboratory experiments and the development of specialized equipment and innovative experimental protocols (experimental study of elastic properties of different constituents of partially saturated argillite using nano-indentation tests; experimental observations of mechanical dilation at the onset of gas flow in Callovo-Oxfordian claystone), as well as the in-situ study of rocks, notably in underground quarries and mines (tests to evaluate the impact of water table fluctuations on the stability of underground chalk quarries; geotechnical observations on construction of waste rock barricades such as cemented paste backfill retaining structures).